

## Optical dephasing in pentacene-doped PMMA under high pressure

Otto Berg and Eric L. Chronister

Citation: *The Journal of Chemical Physics* **106**, 4401 (1997); doi: 10.1063/1.473482

View online: <http://dx.doi.org/10.1063/1.473482>

View Table of Contents: <http://scitation.aip.org/content/aip/journal/jcp/106/11?ver=pdfcov>

Published by the [AIP Publishing](#)

---

### Articles you may be interested in

[Optical coherence and theoretical study of the excitation dynamics of a highly symmetric cyclophane-linked oligophenylenevinylene dimer](#)

*J. Chem. Phys.* **124**, 194904 (2006); 10.1063/1.2196041

[Double-resonance versus pulsed Fourier transform two-dimensional infrared spectroscopy: An experimental and theoretical comparison](#)

*J. Chem. Phys.* **121**, 5935 (2004); 10.1063/1.1778163

[Optical dephasing in doped organic glasses over a wide \(0.35–100 K\) temperature range: Solid toluene doped with Zn–octaethylporphine](#)

*J. Chem. Phys.* **116**, 8959 (2002); 10.1063/1.1473196

[A photon echo study of two-level systems in polyisobutylene under high pressure](#)

*J. Chem. Phys.* **116**, 1737 (2002); 10.1063/1.1429656

[Pressure-induced dynamics in solid n -alkanes as probed by optical spectroscopy](#)

*J. Chem. Phys.* **108**, 1830 (1998); 10.1063/1.475560

---



# 2014 Special Topics

**AIP | APL Materials**

**Submit Today!**

# Optical dephasing in pentacene-doped PMMA under high pressure

Otto Berg and Eric L. Chronister<sup>a)</sup>

Department of Chemistry, University of California, Riverside, California 92521

(Received 8 November 1996; accepted 11 December 1996)

Pressure- and temperature-dependent photon echo results are obtained for pentacene doped polymethyl methacrylate (PMMA). A unique pressure effect is observed in which the optical dephasing rate increases as the pressure is increased from ambient pressure to 4 kbar, above which the optical dephasing rate is pressure independent up to 43 kbar. The present results are also compared with pressure- and temperature-dependent photon echo results for rhodamine 101 in PMMA, in which the optical dephasing rate was completely insensitive to pressure over the range 0 to 30 kbar. A negative correlation is also observed between the optical dephasing rate and the spectral hole burning efficiency. Line broadening due to pressure induced spectral diffusion may be responsible for both the increased dephasing rate and the reduced spectral hole-burning at high pressure. © 1997 American Institute of Physics. [S0021-9606(97)50411-9]

## INTRODUCTION

The mechanisms of optical dephasing in mixed molecular crystals have been well studied and pentacene has served as an almost ideal substitutional defect chromophore in various host crystals. For example, low-temperature photon echo measurements have been used to document the importance of librational modes in dephasing the pure  $S_1-S_0$  electronic transition of pentacene impurities.<sup>1,2</sup> Theoretical treatments have successfully modeled the temperature dependent dephasing of dilute mixed solids as collections of independent optical two-level systems<sup>3,4</sup> coupled to thermally excited “external” oscillators (librations, acoustic phonons, etc.). Theories have also been developed to account for coupling among chromophores in concentrated samples. Such systems have been treated as collections of dimers<sup>5,6</sup> and as exciton-type impurity bands,<sup>7-9</sup> where the role of static intermolecular disorder at absolute zero temperature is emphasized. For example, delocalization of the electronic excitation on the impurity species is observed to increase homogeneous optical dephasing rates of pentacene dimers<sup>10</sup> as well as for pentacene monomers at high concentration.<sup>11</sup>

In contrast to mixed crystals, the status of both theory and experiment for doped *amorphous* solids is less satisfactory. Whereas pure dephasing processes in crystals freeze out below  $\sim 5$  K, doped glasses show residual temperature-dependent pure dephasing down to the lowest temperatures studied.<sup>12</sup> It is generally supposed that the fluctuations responsible for the anomalous thermal properties of pure glasses (“tunneling two-level systems”) are also involved in the optical dephasing of chromophores doped into glassy solids. As was the case with crystals, pentacene is also among the most thoroughly studied organic dopants in organic glasses. Molenkamp and Wiersma reported a discrepancy between the homogeneous linewidth of pentacene in polymethylmethacrylate (PMMA) obtained from accumulated photon echo versus hole-burning measurements.<sup>13</sup> This difference was attributed to spectral diffusion and highlighted the role

of the experimental timescale. A hole-burning study on pentacene doped PMMA was published by van den Berg and Völker,<sup>14</sup> and together with the recent results of Meijers and Wiersma, quantitative agreement between the photon echo and spectral hole-burning techniques has been reached.<sup>15</sup> At 1.7 K, the dephasing rate measured by means of two-pulse echoes ( $10^{-10}$  s observation) merges smoothly with the result from non-photochemical hole-burning (100 s observation), due to spectral diffusion in the period  $10^{-9}$  to  $10^{-5}$  s.<sup>15</sup>

The dependence of the optical dephasing rate on “waiting time” has been formalized in terms of a distribution of fluctuation rates. Due to the non-equilibrium nature of glassy materials, a broad distribution of nearly equal energy configurations of the solid gives rise to dynamic tunneling processes even at liquid helium temperatures. Furthermore, a hyperbolic distribution of dynamic rates is found to be consistent with the form of optical dephasing results.<sup>16,17</sup> More relevant to the present study is the nature of the coupling between the doped chromophore and fluctuating TLS of the host glass. Various formal methods have found that only weak dipole-dipole coupling produces exponential echo decays. Simple distributions of tunneling system parameters yield the ubiquitous  $T^{1.3}$  dependence of low-temperature linewidths.<sup>18-20,13,21</sup> An identical temperature power law has also been derived assuming a distribution of tunneling asymmetry parameters.<sup>22</sup> Although microscopic models are seriously underdetermined by experiments that average over a variety of local structures, coupling strengths, etc., some of these limitations have recently been addressed by studies of single chromophores<sup>23,24</sup> and ensembles of identical systems in amorphous hosts (e.g., protein bound chromophores in glasses). The present strategy is to distort both the chromophore-host coupling and the relevant TLS distributions of the host in a well-defined way using static high pressure, and to investigate the resulting changes in optical dephasing by temperature-dependent photon echo measurements.

In the present study, pentacene-doped PMMA at pressures up to 43 kbar is characterized by absorption, emission, and photon-echo spectroscopies. We are particularly inter-

<sup>a)</sup> Author to whom correspondence should be addressed.

ested in the pure optical dephasing rate, which is controlled by elementary interactions of the chromophore with its environment. At temperatures greater than 5 K this interaction is typically dominated by thermally active optical phonons of the glass. Since compression typically leads to increased vibrational energies, previous high pressure experiments have confirmed that compression tends to reduce thermal dephasing due to a decrease in the corresponding phonon occupation.<sup>25–27</sup> In the present high pressure study we focus on the low-temperatures region between 1 and 3 K, at which dephasing is expected to be dominated by TLS fluctuations unique to glasses. We find that the homogeneous dephasing rate increases with pressure up to about 4 kbar, after which the system is relatively insensitive to further pressure increases up to 43 kbar. Both of these results are intriguing given the significant compression of the matrix and the resulting changes in electronic and vibrational energies over the 4 to 43 kbar region. The present results are also compared and contrasted with recent photon echo measurements on rhodamine 101 in the same PMMA matrix,<sup>28</sup> in which the optical dephasing rate was observed to be independent of pressure from 1 atm up to 30 kbar.

## EQUIPMENT AND PROCEDURES

### Sample preparation

The photon echo experiments were performed on samples  $\leq 0.3$  mm thick with an optical density  $\sim 0.3$ . Due to its low solubility, pentacene is difficult to incorporate into PMMA films of good optical quality. In the present study these difficulties were addressed by photochemically generating pentacene monomers *in situ*. PMMA films were doped with *s*-dipentacene, a stable, readily soluble precursor which was then photochemically dissociated into pentacene monomers.

*S*-dipentacene is a symmetric dimer of pentacene molecules covalently bound at the central carbon atoms (positions 6 and 13). The aromaticity of the central rings is lost, leaving four naphthalene groups rigidly bound in a paddle-wheel shape. *S*-dipentacene can be photochemically synthesized by irradiating a solution of pentacene in 1-chloronaphthalene with the visible output of a high-pressure mercury lamp; *s*-dipentacene precipitates directly from the solution.<sup>29</sup> This product can be spectroscopically confirmed to be the pure symmetric isomer and was provided to us by Gary Scott.<sup>29</sup> The dipentacene was dissolved in dichloromethane with purified PMMA (Aldrich, average molecular weight 30 000), poured into molds on a glass plate, and allowed to dry slowly. The resulting films were approximately 0.3 mm thick, with a final dipentacene concentration that ranged from 0.01 to 0.02 M. The films were stored at ambient temperature, in air, in the dark.

The near-ultraviolet output of a filtered mercury vapor lamp (nominally 365 nm) was used to photolyze dipentacene within the films. Irradiation by diffuse light for 30 to 45 minutes gave the desired concentration of pentacene monomers. Freshly photolyzed samples were placed directly into a cryostat, or stored at 77 K in the dark between experiments,

since exposure to air and light at room temperature led to degradation of the pentacene (on a timescale of hours).

High pressures were generated in a diamond anvil cell of Merrill–Bassett design.<sup>30</sup> Unphotolyzed, dipentacene-doped PMMA was first pressed into a pre-formed Inconel gasket. The sample was irradiated, then sealed between the diamonds. A chip of synthetic ruby was enclosed with the sample, and another was mounted on the outside of the pressure cell as a reference. Experimental pressures were calculated from the frequency shift of  $R_1$  fluorescence from the ruby with an accuracy of  $\pm 1$  kilobar. Below 4 kbar the calibrated spectral shift in the  $S_1 \leftarrow S_0$  absorbance of pentacene itself was used as a more sensitive pressure scale. The frequency shift in this range was linear in pressure (see Discussion) and accurate to within  $\pm 0.3$  kbar. Ambient pressure is referred to as “0 kbar.” Once loaded into a pressure cell, no degradation of the pentacene was observed under any conditions.

All of the results reported in this study were obtained from samples immersed in a liquid helium bath cryostat, either as bits of film cemented to the sample holder (ambient pressure) or enclosed in a diamond anvil cell. Temperatures below 4.2 K were reached by pumping on the liquid helium, and measured by means of the He vapor pressure. Pressures in the range 0.5 to 18 Torr (1.2–1.9 K) were measured with an oil manometer with an accuracy of  $\pm 0.03$  K. In the range 18–200 Torr (1.9–3.0 K) vapor pressure was measured with a mechanical gauge with an accuracy of  $\pm 0.1$  K. Absorbance spectra were recorded in helium at its normal boiling point, 4.2 K.

### Optical measurements

The light incident on the sample was modulated by a mechanical chopper and the transmitted or emitted light was dispersed through a 0.75 m Spex monochromator and detected with a cooled photomultiplier tube (Hamamatsu R955P). A lock-in amplifier detected the modulated component of the photomultiplier’s output, which was digitized and stored on a personal computer. Fluorescence and fluorescence depolarization decays were obtained using a 400 MHz digitizing oscilloscope (HP 54502A) with appropriate deconvolution of the instrument response function.

The excitation pulses for photon-echo experiments were generated by pumping a cavity-dumped dye laser with the frequency-doubled output of a mode-locked, *Q*-switched, Nd:YAG laser (Quantronix 116) operating at a repetition rate of 800 Hz. The dye laser pulse autocorrelation duration was typically 30–40 ps, with a coherence time of 1 ps. The cavity dumped pulse energies were  $\sim 10 \mu\text{J/pulse}$  and an intracavity prism plus a narrow-gap etalon yielded a frequency bandwidth of  $4 \text{ cm}^{-1}$ . Since intense pulses are known to complicate photon echo experiments in general,<sup>31</sup> and the pentacene/PMMA system in particular,<sup>15</sup> the laser was attenuated until photon echo decays were no longer affected. The experimental energies were  $< 30 \text{ nJ/pulse}$ , measured by a photodiode calibrated against a short-pulse joulemeter (Moletron).

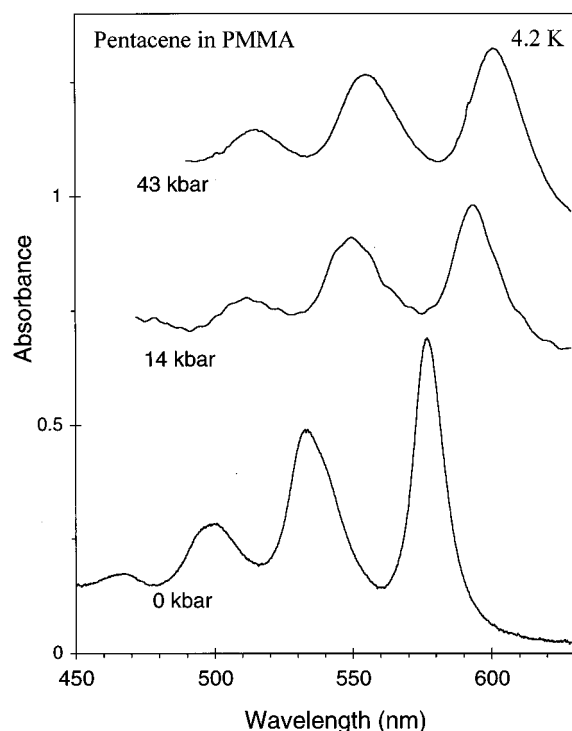


FIG. 1. Absorption spectra of pentacene in PMMA at various pressures. The samples were generated by the room temperature photolysis of *s*-dipentacene doped PMMA.

Two-pulse photon echoes were generated by splitting the dye laser output into two beams of equal intensity. The two beams were focused into the sample, after which the resulting echo signal was collimated, spatially isolated with an iris, and directed into a monochromator (to remove incoherent, broadband emission). The photon-echo signal was identified by its dependence on both excitation pulses and their time ordering. A computer controlled optical delay line and an analog-to-digital converter was used to store the lock-in amplified echo intensity as a function of probe pulse delay. Between 20 and 100 consecutive scans were averaged for each decay reported here.

## RESULTS

### Absorbance

The spectra of dipentacene-doped PMMA were recorded prior to photolysis at room temperature. The films were completely transparent in the wavelength range 700 nm to 400 nm. A monotonically increasing absorbance appeared at shorter wavelengths, making the samples effectively opaque below 285 nm. Superimposed on this signal was a single resolved feature (FWHM 5 nm) centered at 328 nm. The wavelength used for photolysis was on the low-energy tail of this feature. The absorbance at 365 nm was approximately 0.05.

Irradiation of the samples at 365 nm produced a characteristic set of eight new bands: a well-resolved shoulder on the near-ultraviolet features described above; three weak fea-

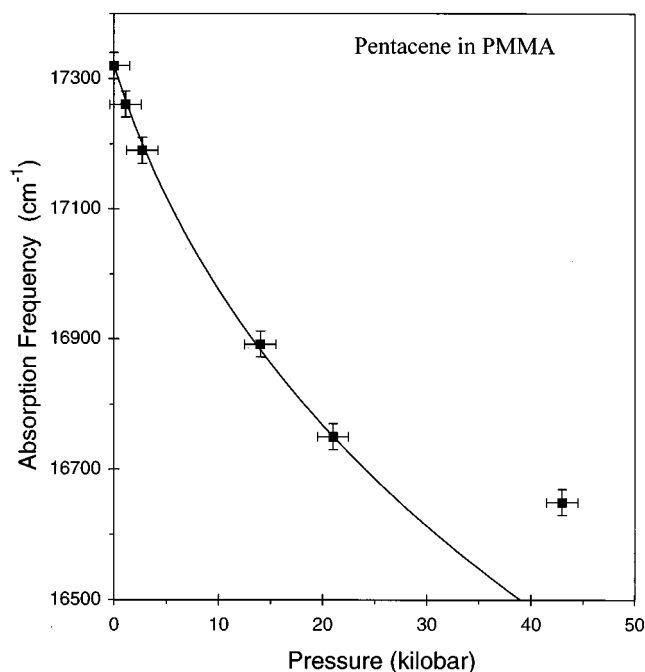


FIG. 2. The pressure-induced shift in the frequency of the absorption maximum of the origin band. The measured shifts (■) are compared with the solid curve obtained by Eq. (3).

tures superimposed on a weak and diffuse background (378 nm, 400 nm, 425 nm); plus an intense, well-resolved quartet (475 nm, 498 nm, 534 nm, 578 nm).

Figure 1 illustrates the effect of pressure on the 450 nm to 600 nm region of the absorption spectrum at 4.2 K. Three spectra were obtained from three different samples used for photon echo measurements. With increasing pressure, the electronic origin and associated vibronic features broaden and shift to lower energy. The absorption maximum of the origin band shifts 24 nm to the red as the pressure is increased from ambient pressure to 43 kbar. However, more than half of this shift is observed by 14 kbar. When the pressure on a sample at high pressure was completely released, the spectral features narrowed and shifted back toward their ambient-pressure positions, but some hysteresis was observed. Following a pressure cycle from 0 kbar to 40 kbar and back to 0 kbar, a residual red-shift of 4 nm and broadening of 2 nm (FWHM) was typical for the lowest-energy band.

Figure 2 summarizes the pressure induced wavenumber shift in the absorption maximum of the electronic origin band over the pressure range 0–43 kbar. The  $-32 \text{ cm}^{-1}/\text{kbar}$  pressure-induced shift observed below 10 kbar is very similar to the shifts reported for hole burning studies at very low pressures.<sup>32</sup> Above 10 kbar the observed spectral shift per unit pressure (i.e., the slope of the data in Figure 2) is significantly reduced due to a decrease in the compressibility of the PMMA matrix.<sup>33</sup> The solid curve in Figure 2 correlates the observed spectral shifts with the square of the density of the surrounding matrix, as discussed in the next section.

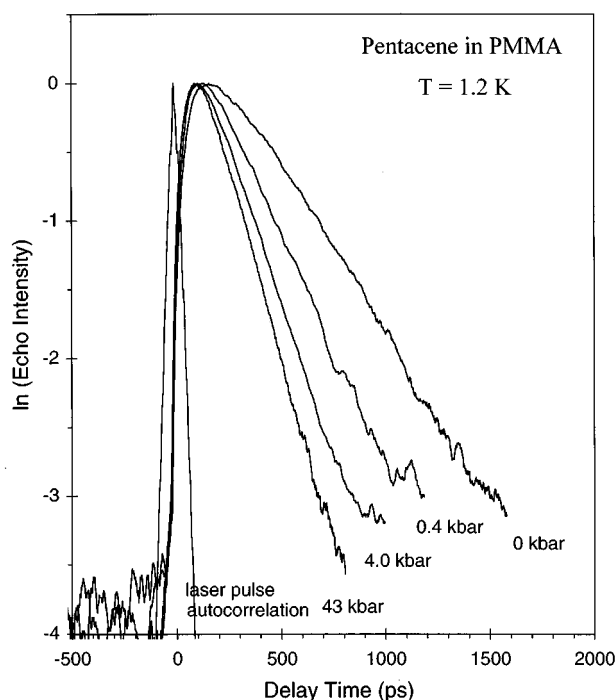


FIG. 3. Selected photon-echo intensity decays at 1.2 K and at various pressures. The effect of increasing pressure on the dephasing rate is dramatically reduced at higher pressures.

### Emission

The effect of pressure on the dispersed emission spectrum at 1.2 K was examined using excitation pulses similar to those used in the photon echo experiments. The line-narrowed emission spectrum (not shown) consisted of sharpened lines ( $\text{FWHM} < 30 \text{ cm}^{-1}$ ) with associated broad sidebands toward lower frequency ( $\text{FWHM} > 100 \text{ cm}^{-1}$ ). Except for the absolute intensity, the shifted spectra were independent of pump position within the absorbance band and they were insensitive to reduction of pump power. The broadband-detected fluorescence decayed exponentially with a time constant of  $14 \pm 2$  nanoseconds at all pressures, consistent with the fluorescence lifetime of pentacene monomers in PMMA.<sup>13</sup> The spectral shift and the bandwidth of the sharp emission features increased monotonically with pressure up to 43 kbar.

### Photon echo

The influence of pressure on the optical dephasing rate is shown in Figure 3. The natural logarithm of the photon-echo intensity is plotted as a function of delay between excitation pulses. Photon echo data at 1.2 K is shown for samples at 0 kbar (ambient pressure), 0.4 kbar, 4.0 kbar, and 43 kbar. The laser pulse autocorrelation trace indicates the practical time resolution of the experiment. For exponential photon echo decays that are much longer than the coherence time of the driving fields, the homogeneous dephasing rate ( $1/T_2$ ) is obtained by<sup>16</sup>

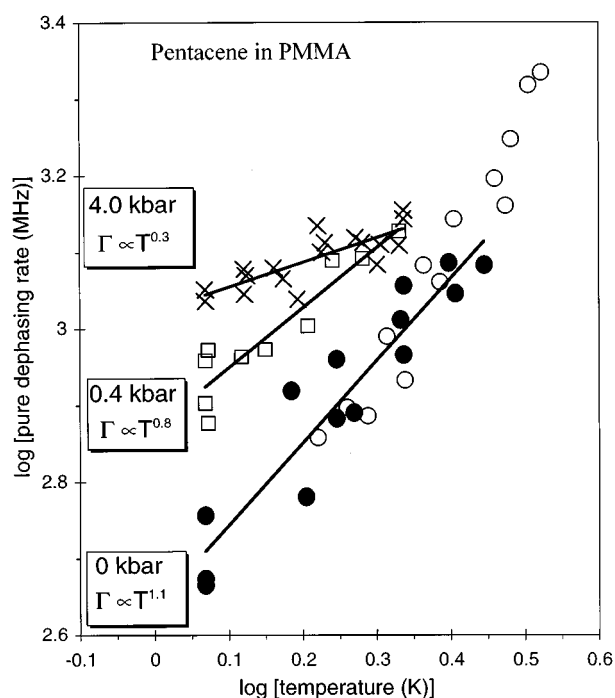


FIG. 4. The effect of temperature and pressure on the pure dephasing rate ( $1/T_2^*$ ). Data acquired at 40 kbar overlapped the data taken at 4.0 kbar.

$$I(\tau) = I_0 \exp\left(\frac{-4\tau}{T_2}\right). \quad (1)$$

The pure dephasing rate ( $1/T_2^*$ ) is obtained by subtracting the contribution from the excited-state lifetime ( $T_1$ ),

$$\frac{1}{T_2} = \frac{1}{2T_1} + \frac{1}{T_2^*}. \quad (2)$$

Using the observed value of the pressure independent fluorescence lifetime  $T_1 = 14 \text{ ns}$ , we obtain pressure-dependent pure dephasing rates at 1.2 K. As the pressure was increased from ambient pressure to 43 kbar we observed a significant increase in the pure dephasing rate  $1/T_2^*$  from 625 MHz (at 0 kbar) to 1450 MHz (at 43 kbar). However, nearly all of the observed change occurs over the range 0 to 4.0 kbar, as shown in Figure 1 and Figure 4.

Figure 4 summarizes the pressure- and temperature-dependent pure dephasing rates ( $1/T_2^*$ ) over the temperature range 1.2 K to 3 K, and for sample pressures of 0 kbar (ambient), 0.4 kbar, 4.0 kbar, and 43 kbar. A log-log plot of the data is presented to facilitate comparison with the power law temperature dependence often observed for optical dephasing in glasses. The ambient pressure results reported by Meijers and Wiersma (open circles)<sup>15</sup> are also included for reference. A variety of temperature dependent photon echo measurements were also obtained at pressures above 4 kbar (up to 43 kbar), however, these results were indistinguishable from the 4 kbar data set shown in Figure 4 (within experimental uncertainty) and were not included in Figure 4 for clarity.

The ambient-pressure data obtained in this study merge smoothly with the higher temperature data of Meijers and Wiersma (which extend to 15 K).<sup>15</sup> At elevated pressure we observe an increase in the pure dephasing rate relative to ambient-pressure samples at the same temperature. The phenomenon is most pronounced at 1.2 K, where the dephasing rate at 4.0 kbar is twice that at ambient pressure. Furthermore, the effect of temperature on the optical dephasing rate at elevated pressures is reduced (i.e., the slope of the  $\log(1/T_2^*)$  versus  $\log T$  data is reduced), corresponding to a power law temperature-dependent dephasing rate with a reduced temperature exponent at higher pressures. Finally, we observe that the system is nearly independent of pressure above 4 kbar (up to at least 43 kbar).

### Spectral hole-burning

Under intense light or extended exposure times, spectral hole-burning occurred, with a corresponding reduction in the magnitude of the photon echo signal. However, at pressures  $\geq 4.0$  kbar spectral hole burning was found to be significantly suppressed. Whereas extended laser exposure could deplete the echo intensity at pressures below 4 kbar, at pressures above 4 kbar only minor decreases in echo intensity were observed even during long exposures. For determinations of the dephasing rate at pressures below 4 kbar the photon-echo data were signal averaged over short time periods to minimize the signal reduction, and no discrepancy was observed between the first and last normalized decays collected.

A significant change in chromophore-lattice interactions at a pressure near 4 kbar is evinced by the change in both the pure dephasing rate and the spectral hole-burning propensity. Below 4 kbar the low-temperature optical dephasing rate increases with pressure up to 4 kbar, and spectral hole-burning is observed at all but the lowest laser powers. In contrast, above 4 kbar the optical dephasing rate is relatively pressure independent and the spectral hole-burning efficiency is significantly reduced.

## DISCUSSION

### Identification of the pentacene photoproduct

PMMA films doped with *s*-dipentacene have a lowest-energy absorbance feature at 348 nm (not shown) that is characteristic of the naphthalene chromophores of *s*-dipentacene.<sup>29</sup> After photolysis at  $\sim 348$  nm, several broad bands appear at visible wavelengths that are characteristic of pentacene in solution.<sup>34</sup> The inhomogeneously broadened low energy absorption bands shown in Figure 1 are attributed to the pure electronic  $S_1(^1A_{1g}) \leftarrow S_0(^1B_{2u})$  transition, plus a progression of higher energy vibronic bands. The frequency separation between the vibronic bands is  $1400 \pm 30$   $\text{cm}^{-1}$ , and the principal vibrational modes responsible for this progression are skeletal C–C stretches plus some C–C–H bending and C–C stretching modes.<sup>35</sup> A similar absorption spectrum (of the first two peaks) for pentacene-doped PMMA

was reported for a sample prepared by pressing solid pentacene into PMMA in a heated hydraulic press.<sup>2</sup>

The site-selected (fluorescence narrowed) emission spectrum (not shown) also corresponds in detail with previously reported emission spectra of pentacene-doped PMMA, as does the 14 ns lifetime measured for the photogenerated samples.<sup>13</sup> All of the spectroscopic analyses of our samples correspond to published spectra for pentacene monomers doped into PMMA. However, we cannot rule out the existence of closely associated pentacene molecules since analogous spectra of distinct pentacene dimers are not available for comparison.

### Pentacene concentration

The concentration of chromophores can be calculated using the Beer–Lambert law for the integrated absorbance,  $\bar{A} = Cl\tilde{\sigma}$ , where  $C$  is the concentration of chromophores,  $l$  is the sample thickness, and  $\tilde{\sigma} = 8\pi^3\nu\mu^2/3nch$  is the integrated molecular cross-section<sup>36</sup> (here  $\mu$  is the magnitude of the transition dipole moment,  $\nu$  is the transition frequency,  $n = 1.5$  is the index of refraction of PMMA,  $c$  is the speed of light, and  $h$  is Planck's constant). The integrated absorption spectrum of pentacene in solution yields an oscillator strength of 0.08,<sup>37</sup> whereas optical free induction and optical nutation measurements yield a transition dipole moment of 1 Debye for the electronic origin transition of one pentacene photosite in crystalline para-terphenyl.<sup>38,39</sup>

In the present study, a direct comparison of the integrated  $S_1 \leftarrow S_0$  absorbance region shown in Figure 1 (i.e.,  $1270 \pm 120$   $\text{cm}^{-1}$  at 0 kbar for  $l = 280$   $\mu\text{m}$ ) with the published absorption spectrum of pentacene in trichlorobenzene solution<sup>34</sup> yielded a concentration of pentacene in PMMA  $C = 5.5 \pm 0.2 \times 10^{-4}$  mole/liter. The sample thickness in the high pressure diamond anvil cell ranged from 100 to 150  $\mu\text{m}$  depending on the gasket. Reduced optical path length accounts for the reduced integrated band area at higher pressures in Figure 1.

### Intermolecular coupling

Because of the photochemical method used to generate pentacene in PMMA, we address the possibility that closely associated pentacene molecules are electronically coupled. It has previously been shown that low temperature (15 K) photolysis of covalent dimers of anthracene and tetracene in PMMA matrices can generate absorption and emission features that are red-shifted (and distorted) relative to the isolated monomer spectrum.<sup>40,41</sup> Such spectral features have been attributed to the formation of closely associated monomer pairs at low temperature (i.e., noncovalent “sandwich dimers”).<sup>40,41</sup> However, even when such “sandwich dimers” are generated (by photolysis at low temperature), temperature cycling from 15 K to 290 K and back to 15 K caused the absorption and emission spectra to revert to those of the unperturbed monomeric species.<sup>40,41</sup> Thus, the mobility of polyacene molecules in PMMA at room temperature allows the migration and separation of the polyacene monomer species following photolysis. In the present study, the

room temperature photolysis of di-pentacene doped PMMA samples yielded absorbance and emission spectra that closely match the spectra reported for pentacene monomers in amorphous hosts. Of course some significant pentacene–pentacene interactions may not reveal themselves in the absorption and/or emission spectra.

### Time-resolved fluorescence depolarization

In cases where intermolecular interactions are not strong enough to affect the absorption and emission spectra, they can still give rise to significant intermolecular energy transfer. Fluorescence depolarization rates were measured to examine the rate of energy transfer between photochemically generated pentacene molecules in PMMA. These results (not shown) showed no evidence of a fast energy transfer contribution that would be expected for closely associated chromophores. Furthermore, the observed time-resolved fluorescence anisotropy decayed with the form  $r(t) = r_0 \exp(-\alpha t^{1/2})$ , which is consistent with a random distribution of chromophores.<sup>42</sup> The fluorescence depolarization results suggest that the pentacene chromophores created by room temperature photolysis of di-pentacene in PMMA behave as relatively unperturbed isolated chromophores.

The effects of weaker interactions and concentration fluctuations may also be reduced by inhomogeneous broadening in PMMA. In mixed crystals, it has been demonstrated that the dephasing rate and photon echo decay function are very sensitive to coupling among *multiple* pentacene molecules, even at concentrations as low as  $5.4 \times 10^{-5}$  mole/liter.<sup>11</sup> However, in an inhomogeneously broadened sample the effective concentration of chromophores resonant at a given frequency is reduced by the extent of inhomogeneous broadening. All other things being equal, the effective resonant concentration would scale inversely with the inhomogeneous bandwidth (observed to be  $\sim 1 \text{ cm}^{-1}$  in the mixed crystal and  $\sim 395 \text{ cm}^{-1}$  in PMMA). When the concentration of our pentacene doped PMMA samples is reduced by this ratio we obtain a value of  $5.5 \times 10^{-4} M/395 = 1.4 \times 10^{-6} M$ , i.e., in the empirical low-concentration limit. Pairwise coupling is more difficult to rule out since the absorption bands associated with  $S_1 \leftarrow S_0$  transitions of pentacene dimers in a crystalline matrix are shifted from the monomer resonance by less than  $40 \text{ cm}^{-1}$ .<sup>10</sup>

Further evidence that delocalized excitations are not playing a significant role in the present pentacene/PMMA system is the convergence of our photon echo measurements of optical dephasing rate with those reported for PMMA directly doped with pentacene.<sup>15</sup> Both measurements yield a pure dephasing rate of  $770 \pm 100 \text{ Mhz}$  at  $1.7 \text{ K}$ , as shown by a comparison of the open and solid circles in Figure 4. Spectral hole-burning results<sup>14</sup> are also in agreement with the stimulated echo results at long waiting times.<sup>15</sup> Since both theory and experiment<sup>7,11</sup> indicate a proportional relation between the dephasing rate of delocalized excitations and the concentration, this level of agreement indicates the absence of such effects.

### Pressure-induced spectral shifts and inhomogeneous broadening

The pressure induced shift in the electronic origin band of pentacene/PMMA at  $14 \text{ kbar}$  is  $-450 \pm 30 \text{ cm}^{-1}$  (shown in Figure 1), corresponding to a shift versus pressure ratio of  $\Delta \tilde{\nu}_p / \Delta p = -32 \text{ cm}^{-1}/\text{kbar}$  over this pressure range. Interestingly, a pressure-dependent spectral hole-burning study in the same system at  $1.5 \text{ K}$  yielded a shift of  $-0.22 \text{ cm}^{-1}$  with an applied pressure ( $\Delta p$ ) of  $0.0068 \text{ kbar}$ ,<sup>32</sup> which corresponds to a similar  $\Delta \tilde{\nu}_p / \Delta p = -33 \pm 2 \text{ cm}^{-1}/\text{kbar}$  ratio even at this very low pressure region. Although the pressure shift is clearly fairly linear below  $14 \text{ kbar}$ , Figure 2 illustrates the reduced spectral shifts at higher pressures (due to a decrease in the compressibility of the PMMA matrix<sup>33</sup>).

The solid curve in Figure 2 is a model which expresses the pressure-induced frequency shift as an extension of the gas-to-matrix solvent shift, assuming that dispersive intermolecular interactions are dominant.<sup>43,44</sup> Specifically, the spectral shift of a non-polar solute (such as pentacene) interacting with a nonpolar matrix (not strictly true of PMMA),  $\Delta \tilde{\nu}$ , is taken to be inversely proportional to the sixth power of the average distance between the chromophore and the surrounding matrix, i.e., proportional to the square of the density.<sup>43,44</sup> Utilizing the gas to solid spectral shift at atmospheric pressure,  $\Delta \tilde{\nu}_0$ , one obtains,

$$\Delta \tilde{\nu} = \Delta \tilde{\nu}_0 \cdot \left( \frac{\rho}{\rho_0} \right)^2 \quad (3)$$

where  $\rho/\rho_0$  is the density relative to that at atmospheric pressure, and  $\Delta \tilde{\nu}$  is the spectral shift with respect to the gas-phase electronic origin ( $\Delta \tilde{\nu} = \tilde{\nu} - \tilde{\nu}_{\text{VAC}}$ ).

The gas-to-PMMA solvent spectral shift for pentacene at atmospheric pressure,  $\Delta \tilde{\nu}_0 = -1305 \text{ cm}^{-1}$ , is obtained from the gas-phase electronic origin of pentacene  $\tilde{\nu}_{\text{vac}} = 18\,625 \text{ cm}^{-1}$ <sup>45</sup> and the peak of the 0-0 absorbance in PMMA at ambient pressure  $\tilde{\nu}_0 = 17\,320 \text{ cm}^{-1}$ . Using the pressure-density relation for PMMA,<sup>33,46</sup> Eq. (3) yields a good fit to the observed spectral shifts at pressures below  $25 \text{ kbar}$ , as indicated by the solid curve in Figure 2. The discrepancy between Eq. (3) and the experimentally observed spectral shifts at higher pressures may be due to a decrease in the compressibility of PMMA at higher pressure (that may not be accurately represented in the  $P$ - $V$  relationship).<sup>33</sup> It is also possible that non-dispersive interactions involving the polar carbonyl groups of PMMA may become more significant at higher pressures.

### Pressure effects on optical dephasing

The pressure-induced changes in the optical dephasing of pentacene in PMMA are unique. Similar temperature and pressure dependent photon echo measurements on rhodamine 101 in PMMA were surprisingly pressure independent over the  $0$  to  $30 \text{ kbar}$  range investigated.<sup>28</sup> In contrast, when the electronic states of the solute interact strongly with low-frequency optical modes of the matrix, the dephasing rate typically decreases with pressure at any fixed temperature.<sup>25–27</sup>

The pressure independent optical dephasing observed above 4 kbar is also inconsistent with electronic coupling to thermally populated low frequency phonon-like modes. It is difficult to explain the insensitivity of the optical dephasing rate of pentacene in PMMA over the 4–43 kbar pressure range, particularly in light of the significant changes in other physical properties of the matrix over the same pressure range. For example, the relative volume of the sample and the density and dispersion of Debye phonons (with corresponding changes in thermal excitation at the relevant temperatures) are curiously detached from the optical coherence phenomena.

There are significant differences between the temperature and pressure effects on the optical dephasing of pentacene versus rhodamine 101 as solute chromophore in a PMMA matrix. While both of these chromophores reveal a general insensitivity of the dephasing rate over wide pressure ranges, the pentacene in PMMA results show two unique aspects: (1) a pressure effect on  $1/T_2^*$  at pressures below 4 kbar; and (2) the accompanying modified power law temperature dependence.

In the present study, the *increase* in the dephasing rate ( $1/T_2^*$ ) observed for a pressure increase from 0 to 4 kbar suggest that something other than electronic coupling to low frequency optical modes (e.g., TLS) is responsible. Furthermore, since the pressure-induced increase in the optical dephasing rate is greatest at low temperature, the power law temperature dependence of the optical dephasing rate becomes very weak at higher pressures.

A  $T^{1.3}$  power law has been reported for the lowest temperature ambient pressure data for pentacene in PMMA.<sup>14,15</sup> Although the present results overlap with these previous ambient pressure results, the best power law fit to our 0 kbar data yields  $(1/T_2^*) \propto T^{1.1}$ . Similarly, the best power law fits for the data at elevated pressures are  $(1/T_2^*) \propto T^{0.8}$  at  $P = 0.4$  kbar, and  $(1/T_2^*) \propto T^{0.3}$  at  $P \geq 4.0$  kbar, as shown in Figure 4. If the temperature exponent of the linewidth,

$$\Gamma \propto T^{1+\Delta} \quad (4)$$

is correlated with the TLS density of states,<sup>16</sup>

$$\rho(E) \propto E^\Delta, \quad (5)$$

then the high pressure results suggest an anomalous density of TLS states that *decreases* with increasing TLS energy, i.e.,  $\Delta < 1$ .

### Effect of pressure on photophysical spectral hole-burning

The spectral hole-burning efficiency of pentacene-doped PMMA was observed to correlate with the pressure effect on  $1/T_2^*$ . Specifically, the efficiency of spectral hole-burning is reduced for pressures  $\geq 4$  kbar, which is the same pressure at which the optical dephasing rate reaches its limiting high pressure value. The similar and restricted pressure region over which these changes are observed suggests a correlation between the factors that determine the hole-burning rate and the optical dephasing rate. van den Berg and Völker provide

evidence that the photophysical product states of pentacene in PMMA lie within 50 GHz ( $1.7 \text{ cm}^{-1}$ ) of the burning frequency,<sup>14</sup> which can be compared to the 3 GHz frequency range accessible by spectral diffusion.<sup>15</sup> A general increase of spectral diffusion under pressure would be sufficient to explain both the accelerated dephasing rate (diffusion on the timescale of the echo experiment) and the reduced hole-burning efficiency (diffusion on the shot-to-shot timescale). Alternatively, the correlation between hole-burning efficiency and the dephasing rate of individual chromophores is also consistent with weaker hole-burning due to increased linewidth of the transitions. One recent comparative study of doped polymers has related hole-burning efficiency to bulk sample density,<sup>47</sup> however, such a correlation is not observed in the present data nor in our previous high pressure photon echo study of optical dephasing of rhodamine 101 in PMMA.<sup>28</sup> Where spectral diffusion data are available at ambient pressure (e.g., a waiting time of  $\sim 3$  ns) its absolute contribution to the linewidth is 300 MHz for pentacene in PMMA<sup>15</sup> versus 120 MHz for rhodamine 101 in PMMA,<sup>17</sup> which may account for the different pressure effects observed for pentacene versus Rh101 in the same PMMA matrix.

Regarding the microscopic basis of dephasing and spectral diffusion, we note that the electronic transition of a dopant is modulated by “external” oscillators only to the extent that coupling between dopant and oscillator is different in the two electronic states involved. A standard result of theoretical impurity/TLS dephasing models is that only dipole–dipole coupling is consistent with observations. Therefore, in considering the difference between pentacene and rhodamine 101 as chromophores, we address the change in dipole moment associated with  $S_1-S_0$ . Rhodamine 101 has an intrinsic permanent dipole moment in both states; for a variety of dyes in polymeric matrices this difference is in the range 0.2–2 D.<sup>48</sup> Both states of isolated pentacene, by contrast, are nonpolar. It is the uncommonly large polarizability of  $S_1$  pentacene that, in the presence of a polar matrix, yields a large change of dipole moment. For pentacene in PMMA, a value of  $\Delta\mu = 1.5$  D has been measured by means of electric field dependent hole burning.<sup>44</sup> In light of the present data, it appears that coupling of TLS to a purely matrix-induced dipole moment change (pentacene) is more sensitive to pressure than coupling to an intrinsic dipole moment change of comparable magnitude (rhodamine 101).

### CONCLUSIONS

Two main comparisons are made between the pressure-dependent photon-echo results for pentacene in PMMA versus those obtained for Rh101 in the same matrix: (1) the optical dephasing rate for Rh101 in PMMA was insensitive to pressure increases over the range 0 to 30 kbar, while pentacene in PMMA showed little change in optical dephasing from 4 kbar to 42 kbar, and (2) the pentacene in PMMA system showed a significant pressure effect, but it was re-

stricted to a small pressure region from 1 atm to 4 kbar, above which it was relatively insensitive to further pressure increases.

The pressure increases up to 4 kbar were also observed to correlate with a decrease in the rate of spectral hole-burning. This correlation suggests that pressure induced spectral diffusion on a very fast timescale may be responsible for the increased dephasing rate. Furthermore, the decrease in spectral hole-burning at high pressure may be due to the corresponding broader spectral linewidth at high pressure.

## ACKNOWLEDGMENT

We acknowledge the National Science Foundation (CHE-9400542) for financial support of this research.

- <sup>1</sup>W. H. Hesselink and D. A. Wiersma, in *Spectroscopy and Excitation Dynamics of Condensed Molecular Systems*, edited by V. M. Agranovich and R. M. Hochstrasser (North-Holland, Amsterdam, 1983).
- <sup>2</sup>L. W. Molenkamp and D. A. Wiersma, *J. Chem. Phys.* **80**, 3054 (1984).
- <sup>3</sup>K. E. Jones and A. H. Zewail, in *Advances in Laser Chemistry*, Springer Series in Chemical Physics, Vol. 3, edited by A. H. Zewail (Springer, Berlin, 1984).
- <sup>4</sup>P. de Bree and D. A. Wiersma, *J. Chem. Phys.* **70**, 790 (1979).
- <sup>5</sup>J. L. Skinner, H. C. Andersen, and M. D. Fayer, *J. Chem. Phys.* **75**, 3195 (1981).
- <sup>6</sup>F. C. Spano and W. S. Warren, *J. Chem. Phys.* **89**, 5492 (1988).
- <sup>7</sup>L. Root and J. L. Skinner, *J. Chem. Phys.* **81**, 5310 (1984).
- <sup>8</sup>W. S. Warren and A. H. Zewail, *J. Phys. Chem.* **85**, 2309 (1981).
- <sup>9</sup>F. C. Spano and W. S. Warren, *J. Chem. Phys.* **90**, 6034 (1989).
- <sup>10</sup>F. G. Patterson, W. L. Wilson, H. W. H. Lee, and M. D. Fayer, *Chem. Phys. Lett.* **110**, 7 (1984).
- <sup>11</sup>R. J. Gulotty, C. A. Walsh, F. G. Patterson, W. L. Wilson, and M. D. Fayer, *Chem. Phys. Lett.* **125**, 507 (1986).
- <sup>12</sup>I. Zschokke-Gränacher, Ed., *Optical Spectroscopy of Glasses* (Reidel, Dordrecht, 1986).
- <sup>13</sup>L. W. Molenkamp and D. A. Wiersma, *J. Chem. Phys.* **83**, 1 (1985).
- <sup>14</sup>R. van den Berg and S. Völker, *Chem. Phys. Lett.* **127**, 525 (1986).
- <sup>15</sup>H. C. Meijers and D. A. Wiersma, *J. Chem. Phys.* **101**, 6927 (1994).
- <sup>16</sup>Y. S. Bai and M. D. Fayer, *Phys. Rev. B* **39**, 11066 (1989).
- <sup>17</sup>L. R. Narasimhan, Y. S. Bai, M. A. Dugan, and M. D. Fayer, *Chem. Phys. Lett.* **176**, 335 (1991).
- <sup>18</sup>J. M. Hayes, R. P. Stout, and G. J. Small, *J. Chem. Phys.* **74**, 4266 (1981).
- <sup>19</sup>S. K. Lyo, *Phys. Rev. Lett.* **48**, 688 (1982).
- <sup>20</sup>D. L. Huber, M. M. Broer, and B. Golding, *Phys. Rev. Lett.* **52**, 2281 (1984).
- <sup>21</sup>D. L. Huber, M. M. Broer, and B. Golding, *Phys. Rev. B* **33**, 7297 (1986).
- <sup>22</sup>R. Jankowiak and G. J. Small, *Chem. Phys. Lett.* **207**, 436 (1993).
- <sup>23</sup>E. Geva, P. D. Reilly, and J. L. Skinner, *Acc. Chem. Res.* (in press).
- <sup>24</sup>J. L. Skinner and W. E. Moerner, *J. Phys. Chem.* **100**, 13 251 (1996).
- <sup>25</sup>A. Ellervee, J. Kikas, A. Laisaar, A. Suisalu, *J. Luminescence* **56**, 151 (1993).
- <sup>26</sup>R. A. Crowell and E. L. Chronister, *Chem. Phys. Lett.* **216**, 293 (1993).
- <sup>27</sup>B. J. Baer and E. L. Chronister, *J. Phys. Chem.* **99**, 7324 (1995).
- <sup>28</sup>B. J. Baer, R. A. Crowell, and E. L. Chronister, *Chem. Phys. Lett.* **237**, 380 (1995).
- <sup>29</sup>T. Yamashita, M.S. thesis, University of California, Riverside, 1990.
- <sup>30</sup>L. Merrill and W. A. Bassett, *Rev. Sci. Instrum.* **45**, 290 (1974).
- <sup>31</sup>R. W. Olson, H. W. H. Lee, F. G. Patterson, M. D. Fayer, *J. Chem. Phys.* **76**, 31 (1982).
- <sup>32</sup>Th. Sesselmann, L. Kador, W. Richter, and D. Haarer, *Europhys. Lett.* **5**, 361 (1988).
- <sup>33</sup>J. R. Asay, D. L. Lamberson, A. H. Guenther, *J. Appl. Phys.* **40**, 1768 (1969).
- <sup>34</sup>E. Clar, *Polycyclic Hydrocarbons* (Academic, London, 1964), p. 425.
- <sup>35</sup>K. Ohno, *J. Mol. Spectr.* **77**, 329 (1979).
- <sup>36</sup>J. T. Yardley, *Introduction to Molecular Energy Transfer* (Academic, New York, 1980).
- <sup>37</sup>H. B. Klevens and J. R. Platt, *J. Chem. Phys.* **17**, 470 (1949).
- <sup>38</sup>T. E. Orlowski and A. H. Zewail, *J. Chem. Phys.* **70**, 1390 (1979).
- <sup>39</sup>H. de Vries and D. A. Wiersma, *J. Chem. Phys.* **70**, 5807 (1979).
- <sup>40</sup>M. A. Iannone and G. W. Scott, *Mol. Cryst. Liq. Cryst.* **211**, 375 (1992).
- <sup>41</sup>M. A. Iannone, R. A. Mackay, G. W. Scott, and T. Yamashita, *Proc. Soc. Photo-Opt. Instrum. Eng.* **1213**, 155 (1990).
- <sup>42</sup>J. Baumann and M. D. Fayer, *J. Chem. Phys.* **85**, 4087 (1986).
- <sup>43</sup>H. C. Longuet-Higgins and J. A. Pople, *J. Chem. Phys.* **27**, 192 (1957).
- <sup>44</sup>Th. Sesselmann, W. Richter, D. Haarer, *Europhys. Lett.* **2**, 947 (1986).
- <sup>45</sup>A. Amirav, U. Even, and J. Jortner, *Chem., Lett.* **72**, 21 (1980).
- <sup>46</sup>P. W. Bridgman, *Proc. Am. Acad. Arts Sci.* **76**, 71 (1948).
- <sup>47</sup>J. Takahashi, J. Tsuchiya, and K. Kawasaki, *Chem. Phys. Lett.* **222**, 325 (1994).
- <sup>48</sup>I. Renge, *J. Opt. Soc. Am. B* **9**, 719 (1992).